

Evidence for the transforming activity of a truncated Int6 gene, *in vitro*

Susan B Rasmussen¹, Edith Kordon², Robert Callahan¹ and Gilbert H Smith^{*1}

¹National Institutes of Health, National Cancer Institute, Laboratory of Tumor Immunology and Biology, 10 Center Drive Room 8B07, Bethesda, Maryland, MD 20892-1750, USA; ²Academia Nacional de Medicina, Buenos Aires, Argentina

Int6/eIF3-p48 was first identified as a common integration site for MMTV in mouse mammary tumors. In all cases, the MMTV integration event resulted in an interruption of the normal Int6 transcript from one allele leaving the second allele intact and operative. We hypothesize that insertion of MMTV into Int6 results in a mutated allele that encodes a shortened Int6 mRNA and protein (Int6sh), which either modifies normal Int6 function or possesses a new independent function. To confirm the transforming potential of the mutation and its dominant function, we transfected two mammary epithelial cell lines, MCF10A (human), and HC11 (mouse), with Int6sh under the control of the elongation factor-1 α (eEF1A) promoter. Expression of Int6sh in MCF10A and HC11 mammary epithelial cells leads to anchorage-independent growth in soft agar indicative of a transformed phenotype. Colonies selected from agar exhibited high levels of mutated Int6sh and wild type Int6 RNA transcripts by RT-PCR and Northern blot analysis. In addition, Int6sh transformed MCF10A and HC11 cells formed nodular growths, *in vivo*, in immune compromised hosts. NIH3T3 cells, mouse embryo fibroblasts, were also transformed to anchorage-independent growth *in vitro* by Int6sh expression. These observations provide direct evidence that the Int6 mutations observed in MMTV-induced tumors and hyperplasia contribute to the malignant transformation of the mammary epithelial cells. *Oncogene* (2001) 20, 5291–5301.

Keywords: Int6; eIF3-p48; transformation; mammary gland; epithelial cells

Introduction

Int6 was identified and cloned from an MMTV-induced premalignant Czech II mouse mammary epithelial outgrowth line, CZZ1, and its subsequent tumors and metastases, as well as in two additional independent tumors found in the mammary glands of MMTV-infected Czech II mice (Marchetti *et al.*, 1995). All Int6 mutations resulted from insertion of full length MMTV DNA, within intron 5 or intron 9 of the Int6

gene, in the opposite transcriptional orientation. This insertional event resulted in transcription of a truncated Int6 mRNA (Int6sh) in all three independent tumors due to a cryptic transcription stop sequence within the U3 portion of the MMTV-LTR.

Recently, Int6 was discovered to be the gene encoding the eukaryotic translation initiation factor 3 (eIF3) p48 subunit (Asano *et al.*, 1997a). Mammalian eIF3 is a complex comprised of at least 10 subunits and plays an integral part in translation initiation. The eIF3 complex is involved in at least three crucial aspects of translation initiation. The first is the dissociation of the 80S ribosomal complex and recruitment of the ternary complex (eIF2-GTP-Met-tRNA) (Hershey, 1991). Second, in association with the eIF4F complex, it is responsible for the binding and alignment of mRNA (Methot *et al.*, 1996; Pestova *et al.*, 1996). Lastly, it appears to regulate the recruitment of eIF5 to the 40S pre-initiation complex (Asano *et al.*, 1999). However, little is known about the manner in which each of the 10 eIF3 subunits interact and bind with each other or to other translation initiation proteins (Asano *et al.*, 1997b).

Transforming or oncogenic properties of translation initiation components have been previously documented. Overexpression of translation initiation factors eIF-4E and eIF4G alone has been shown to transform NIH3T3 cells *in vitro*. Subsequently, rat embryo fibroblasts were also transformed in collaboration with v-myc or E1A (Fukuchi-Shimogori *et al.*, 1997; Lazaris-Karatzas *et al.*, 1990; Lazaris-Karatzas and Sonenberg, 1992). Both eIF3 subunits p40 and p48 are required for binding to the 40S translation preinitiation complex in eukaryotic cells, however whether these two translation initiation factors directly interact with one another is unknown. Amplification and mRNA overexpression of the eIF3p40 gene is associated with breast and prostate cancer (Nupponen *et al.*, 1999). Nupponen *et al.* (2000) eIF3-p40 to chromosome 8q23-24, relatively close to Int6/eIF3-p48, which lies at 8q22-23. Recurrent genetic aberrations have been detected in chromosome regions 8q21 and 8q23-24 and are linked to breast and prostate cancer. The chromosomal localization of eIF3 subunits p40 and p48 near one another as well as their potential involvement in breast cancer may be of significance.

In the present work, we demonstrate that expression of a truncated Int6 gene (Int6sh), in the presence of two fully competent copies of wild type Int6 gene, is

*Correspondence: GH Smith; E-mail: gs4d@nih.gov
 Received 24 January 2001; revised 26 April 2001; accepted 8 May 2001

sufficient to transform the growth properties of both mammary epithelial cells and NIH3T3 cells *in vitro*.

Results

Human (MCF10A) and mouse (HC11) mammary epithelial cell lines were utilized as target cells for assessing the effects of Int6sh expression on anchorage-dependent and anchorage-independent growth *in vitro*. Transplantation of the Int6sh transfected cell lines into murine host mammary fat pads was used to ascertain whether the Int6sh-transformed cells were capable of producing either hyperplastic or malignant epithelial outgrowths in mice.

The Int6sh RNA transcript is 660 bp long as compared to 1.5 kb full length Int6 transcript (Figure 1). A truncated form of Int6 was selected because the MMTV-induced mutations found in three independent tumors expressed a shortened Int6 RNA transcript. A severely truncated form of the Int6 message was also selected because it represented the shortest of all the truncations caused by MMTV DNA insertion within introns of the Int6 gene in these tumors and was therefore considered the most likely to produce an independent phenotype.

To determine whether our Int6sh and Int6 wild type expression constructs were capable of producing the predicted protein products *in vitro*, they were tested in Promega's TnTTMT7 coupled *in vitro* transcription/translation system using both reticulocyte or wheat germ lysates. In each of these systems appreciable

levels of Int6 wild type (52 kDa) and truncated Int6 (14 kDa) protein were produced. Premature translation termination was ruled out as the hemagglutinin (HA) tag at the C-terminus of the Int6 wild type and truncated Int6 protein was precipitated with both monoclonal and polyclonal HA antibodies. An identical size product was identified as well by an antibody raised against an Int6 specific peptide representing an N-terminal domain common to both Int6sh and Int6 wild type (Figure 2). This demonstrated that the

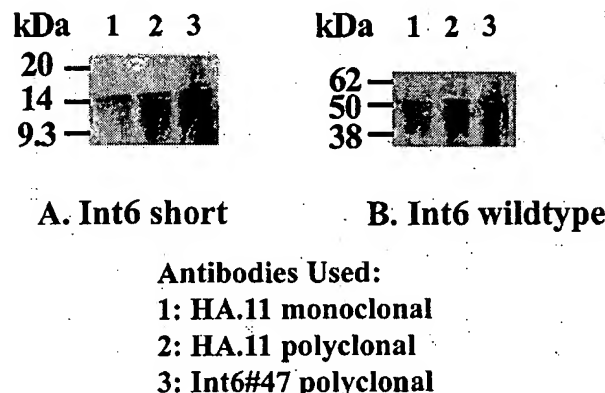


Figure 2 *In vitro* translation and immunoprecipitation of Int6 short and Int6 wild type. Equal amounts (1 µg) of Int6sh and Int6 wild type vectors were *in vitro* translated with [³⁵S]Methionine and then immunoprecipitated with three antibodies, as noted, utilizing protein G agarose. The HA.11 antibodies recognize the C-terminal hemagglutinin epitope tag and the Int6 #47 antibody recognizes the N-terminus of Int6

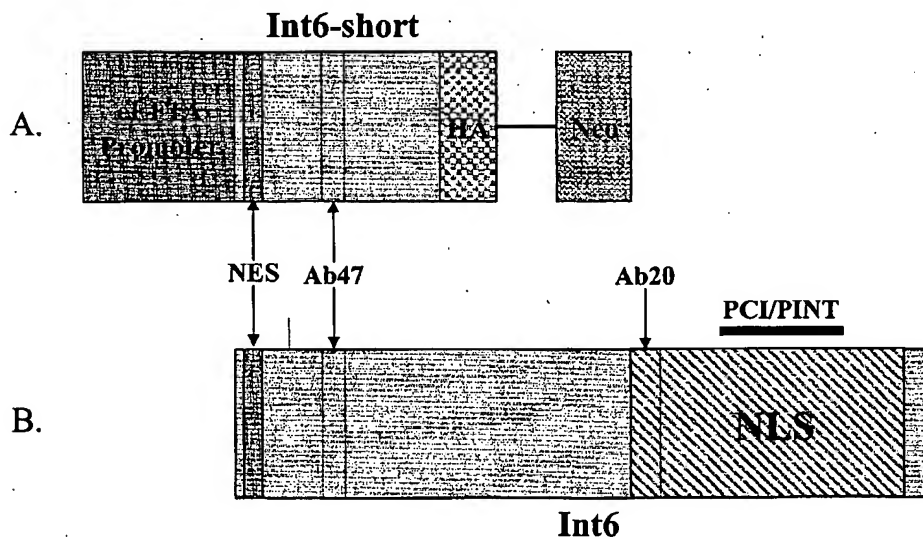


Figure 1 Int6 short transfection vector and motifs. To express truncated Int6, a vector was constructed from the pCDNA 3.1(+) backbone, replacing the cytomegalovirus (CMV) promoter with elongation factor 1-alpha (eEF1A) promoter and adding a hemagglutinin (HA) epitope tag for protein identification purposes. (a) Int6sh-pCEFLHA vector. (b) Int6 localization motifs. Int6/eIF3-p48 contains two cellular localization signals, a bipartite nuclear localization signal and a nuclear export signal (NES) (Guo and Sen, 2000). The nuclear localization signal is located towards the C-terminus (amino acids 264–445) of Int6/eIF3-p48 while the NES is located near the amino terminus (leucines 6, 14 and 18). The Proteasome-COP9 complex Initiation (PCI) and Proteasome-Int6-Nip1-Trip15 (PINT) motifs are located at amino acids 328–407 and 328–391 respectively. The epitope of antibody #47 (Int6 #47) is located at the N-terminus of Int6 (amino acids 58–73) while antibody #20's epitope is found near the center of the Int6 protein (amino acids 265–284). Thus, Int6 #20 antibody does not recognize the Int6sh protein (amino acids 1–137)

constructs produced the predicted full-length Int6sh and Int6 wild type proteins. Using equal amounts of both constructs in the *in vitro* translation reaction, we found that both constructs can be translated simultaneously (data not shown), thus, one message does not preclude the other being translated *in vitro*. Both reticulocyte and wheat germ lysates produced similar results. This was important because Int6 has been reported to be a member of the eIF3 translation complex and we wished to rule out any interference with Int6sh mRNA translation initiation.

In vitro transformation of mammary cell lines

The amino acid sequence of human and mouse Int6 proteins are identical (Miyazaki *et al.*, 1995, 1997). Therefore, the human mammary epithelial cell line, MCF10A, and mouse mammary epithelial cell line, HC11, were chosen as targets because these cells are of mammary origin and exhibit anchorage dependent growth properties *in vitro* and are non-tumorigenic *in vivo*. Stable cell lines expressing Int6sh and Int6 wild type were generated by transfection of the Int6sh/pCEFLHA or Int6 wild type/pCEFLHA constructs using standard liposomal reagents into MCF10A, HC11 or NIH3T3 cells followed by neomycin selection. All of these cell lines produced stable populations that were positive for expression of the full-length mRNA when tested by RT-PCR or Northern blot (not shown). To ascertain whether overexpression of the Int6sh gene would affect the growth properties of MCF10A, HC11 and NIH3T3 cells, soft agar growth assays were performed (MacPherson and Montagnier, 1964). Cells were seeded into soft agar and allowed to grow for 6 weeks. Harvey Ras-transformed MCF10A cells (MCF10AneoT), which have been shown to form colonies in soft agar (a kind gift from Dr David Salomon, LTIB, NCI, USA), were used as a positive control for growth in soft agar (Ciardiello *et al.*, 1990a 1992; Normanno *et al.*, 1994). Int6sh transfected MCF10A cells produced a larger number of colonies compared with MCF10A cells and were found to be equivalent in colony-forming ability with the Harvey Ras-transformed MCF10A cells (MCF10AneoT) (see Figure 5). In separate growth rate studies on plastic, a slight increase in the proliferation rate was observed for the Int6sh-transformed MCF10A cell line as compared to the MCF10A cells (data not shown). The largest colonies in soft agar were isolated and analysed for Int6sh expression by RT-PCR and Northern blot analysis. A high level of the Int6sh transcript was detected in all clones chosen by soft agar growth capability indicating a strong correlation between the acquisition of anchorage independent growth and Int6sh expression (not shown). Preliminary observations on MCF10A cells transfected with full length Int6 indicate that increased expression of wild type Int6 protein does not promote growth in soft agar. These clones were then analysed for Int6sh protein expression. Despite the presence of abundant Int6sh transcript, efforts to detect Int6sh protein

expression by Western blot analysis of either Int6sh transfected HC11, MCF10A or NIH3T3 cells proved unsuccessful, although detection of Int6 wild type was readily apparent. To investigate Int6sh protein expression directly within the transformed cells, we constructed an eEF1A-driven Int6sh vector tagged with a C-terminal green fluorescent protein (GFP) fusion partner. Both MCF10A and NIH3T3 cells transfected with this construct (eEF1AInt6sh/GFP), expressed high levels of Int6sh message after selection in G418 and exhibited readily detectable levels of Int6sh/GFP protein within the transfected cells. These cell lines were stable for expression of the vector. The amount of Int6sh-GFP varied from cell to cell suggesting that the intracellular rates of Int6sh turnover may vary, perhaps with the cell cycle. Nevertheless, these results indicate that as expected Int6sh protein is translated and appears to mainly localize to the cytoplasm since it lacks the nuclear localization signal found towards the C-terminus of Int6 wild type and missing in Int6sh (Figure 3). Western blots of protein extracts from these cells also proved insufficient for detection of the Int6sh protein. Stable transfection of MCF10A and NIH3T3 cells with eEF1AInt6 wild type/GFP also led to the expression of GFP-positive Int6 wild type. Int6 wild type/GFP expression was found in both the cytoplasm and nucleus of the transfected cells and was detectable by Western blotting in cell extracts (not shown). Thus, detection and localization of the Int6sh protein is dependent upon the sensitivity of the method of detection. This supports the hypothesis that the Int6sh protein may have a short half-life in transformed mammalian cells. Wild type Int6 protein was detected in Western blots of extracts from both non-transformed and Int6sh-transformed cells. In the Int6sh-transformed cells the steady state levels of wild type Int6 protein appear to be increased compared to matching non-transformed cells (Figure 4). Additional evidence for a steady state increase in Int6 wild type mRNA expression was also apparent in Northern blots of Int6sh transfected MCF10A cells (not shown). Int6 wild type mRNA migrates at approximately 1.5 Kb and higher levels of Int6 wild type transcript were seen in Int6sh transfected cells when compared to MCF10A and MCF10AneoT cells.

Similar results were obtained when we transfected Int6sh into either HC11, mouse mammary epithelial cells or NIH3T3 fibroblasts. A high level of Int6sh transcript was detectable in the stable transfectants by both RT-PCR and Northern blot analysis (data not shown) and the Int6sh transfected HC11 cells exhibited a significant ability to form colonies in soft agar compared to HC11 cells alone (Figure 5). To determine whether truncated Int6sh-transforming capacity was effective in non-epithelial cell cultures, we transfected NIH3T3 mouse embryo fibroblasts. Int6sh-transfected NIH3T3 cells grew slightly faster than non-transfected cells on plastic (data not shown) and exhibited anchorage independent growth in soft agar (Figure 5). Doubly-transformed DBL/NIH3T3 (DBL, clone 1, K-Ras, SV40T-transformed NIH3T3) cells were pro-

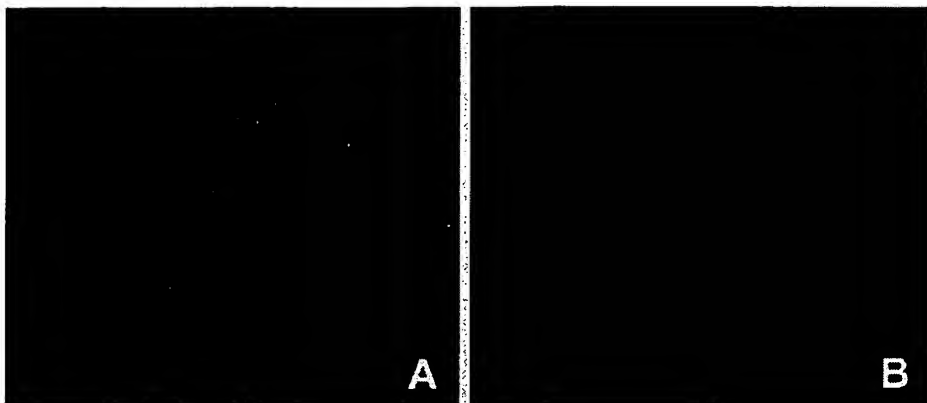


Figure 3 Detection of Int6sh-C-terminal green fluorescent fusion protein. Int6sh-CTGFP/NIH3T3 cells (a) and pCDNA3.1/CT-GFP(no insert)/NIH3T3 cells (b) were grown upon 22 mm square (No.1.) coverslips and fixed in 3.5% paraformaldehyde. Cells were stained with a monoclonal antibody to GFP followed by a FITC-conjugated secondary antibody. DAPI was included to identify the nucleus. Images were taken utilizing standard fluorescence microscopy filters on a Nikon Eclipse TE300 microscope with a 100 \times objective. Int6sh/CTGFP/NIH3T3 cells, one shown in (a) expressed readily detectable levels of Int6sh?GFP protein identified by the green fluorescence. The location of the stain is predominantly cytoplasmic. (b) shows the background level for autofluorescence in the non-expressing NIH3T3 cell transfected with vector alone



Figure 4 Western blot analysis of Int6 protein expression in MCF10A cells. Lanes 1–8 are from several individual stable transfectants of Int6sh/MCF10A cells. MCF10A cells were used as a negative control in the lane 9. Protein lysates (15 μ g) were subjected to SDS-PAGE and then transferred onto nitrocellulose membrane. The membrane was incubated with Int6 #20 polyclonal antibody (1:1000) (Diella et al., 1997) and immunocomplexes were visualized as described in Materials and methods. Full-length Int6 protein migrates at 52.2 kDa. The blots were also reacted with Int6 #47 polyclonal antibody with identical results for Int6 wild type, however Int6sh protein was not detected although the #47 epitope is present on both Int6 wild type and Int6sh (see Figure 2)

vided by Dr David Salomon, LTIB, NCI as a positive control for anchorage independent growth of 3T3 cells in soft agar (Ciardiello et al., 1990b). Anchorage independent growth of the transformed NIH3T3 cells was also associated with high levels of Int6sh mRNA expression. Thus the correlation between anchorage independent growth and high levels of Int6sh RNA expression obtained in mammary epithelial cells extends to NIH3T3 fibroblast cells.

Growth of Int6sh-transfectants in vivo

To assess their tumorigenic potential, Int6sh transfected cell lines were transplanted into athymic (nu/nu) mice (Tables 1 and 2). A total of three *in vivo* experiments were done using the Int6sh/MCF10A cell lines with a minimum duration of 3 months (Table 1). In the first experiment, transplants of 2×10^6 cells/injection were injected into the scapular fat pad with

Matrigel. The appearance of one nodule containing Int6sh transfected MCF10A cells was detected after 3 months. This epithelial nodule was sectioned at 50 μ m step intervals and mounted onto slides. The intervening sections were pooled for DNA extraction and PCR analysis for the presence of human Alu sequences within the epithelial nodule. Alu sequences were found and confirmed that the epithelial nodule was of human and not of mouse origin (Figure 6) (Jurka and Milosavljevic, 1991). In the second experiment, transplants of 2×10^6 cells/bolus were injected subcutaneously near the inguinal mammary fat pads. These inoculations did not yield any epithelial nodules in either MCF10A cells or Int6sh transfected MCF10A cells (Table 1). In the third experiment, a 5 \times larger number of transformed and control cells (1×10^7 cells) was inoculated subcutaneously within the inguinal mammary gland. Epithelial nodules were detected in seven out 15 transplants (47%) (Table 1). Implantation of 5 mg diethylstilbestrol pellets (20% diethylstilbestrol/80% cholesterol) to increase the level of estrogenic stimulation of mammary epithelial growth over the duration of transplantation had no discernible effect on the number of outgrowths within the mammary gland (Table 1 footnote). These transplant experiments demonstrate that these Int6sh transfected MCF10A cells can grow *in vivo* and exhibit a transformed phenotype *in vitro*.

In the first experiments, two million cells were inoculated and only one nodule was found out of 10 implants and this was confirmed to be of human origin. In the second set of inoculations, 10 million cells were implanted, in this experiment a significant number of growths were observed for the transformed Int6sh/ MCF10A cells. Diethylstilbestrol pellets were placed in five recipients in each group of 15 experimental and control. This was done to promote mammary epithelial cell growth, however no significant increase

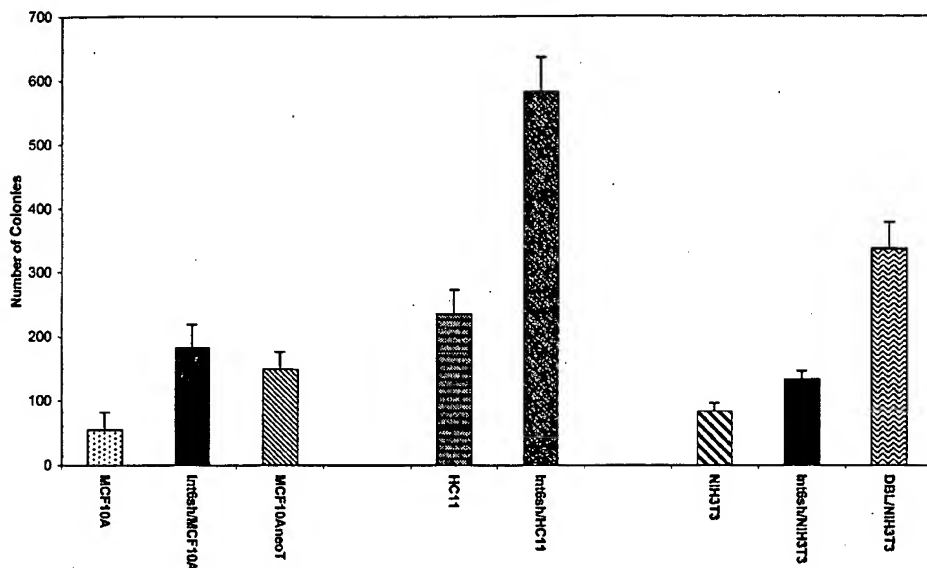


Figure 5 Soft agar colony analysis. Soft agar colonies were plated at a density of 30 K per well in semi-solid media, as described in Materials and methods, for MCF10A, HC11 and NIH3T3 cell lines. These soft agar cultures were incubated for 6 weeks then stained and counted. Colony numbers (at least five separate samples), ≥ 0.1 mm, are plotted versus cell type. Doubly-transformed DBL/NIH3T3 cells and Harvey Ras-transformed MCF10A cells (MCF10AneoT) were provided by Dr David Salomon, LTIB, NCI as a positive control for anchorage independent growth in soft agar (Ciardiello *et al.*, 1990a,b 1992; Normanno *et al.*, 1994)

Table 1 Int6sh/MCF10A *in vivo* transplantation experiments^a

	Subcutaneous inoculation-1 ^b MCF10A	Subcutaneous inoculation-1 ^b Int6sh/MCF10A	Direct fat pad inoculation ^c MCF10A	Direct fat pad inoculation ^c Int6sh/MCF10A	Subcutaneous inoculation-2 ^d MCF10A	Subcutaneous inoculation-2 ^d Int6sh/MCF10A
Number of mice	10	10	10	15	10	15
Number of growths	0	1	0	0	0	7

^aNo growths were seen with MCF10A cells alone. Ten control mice were utilized in each experiment. ^bSubcutaneous injection of 2×10^6 cells in 50:50 media/Matrigel solution was done directly into the scapular fat pad of nude mice. ^cInjection of 2×10^6 cells was done into the right inguinal mammary gland of nude mice. ^dInjection of 1×10^7 cells was done subcutaneously bilaterally near the inguinal mammary glands of nude mice. Five growths were found in mice without diethylstilbestrol pellets and two growths were seen in mice with diethylstilbestrol pellets

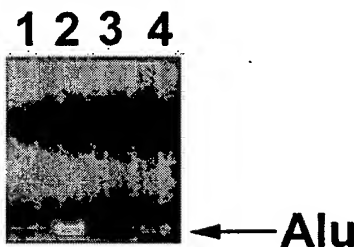


Figure 6 PCR Analysis of *in vivo* growths. Genomic DNA was extracted from paraffin embedded tissue and analysed for human Alu sequences. Mouse Cot-1 DNA (Lane 1) was used as negative control and Human Cot-1 DNA (Lane 2) as the positive control. A double-distilled H₂O sample (Lane 3) was included to rule out contamination. Lane 4 contains DNA extracted from an epithelial growth caused by subcutaneous inoculation of Int6sh transfected MCF10A cells into the scapular fat pad of a nude mouse

in the incidence of positive growth (2/5 with DES versus 5/10 without DES) in the Int6sh-transformed MCF10A cell implants. No *in vivo* growth was found at either concentration of cells or with diethylstilbestrol

Table 2 Int6sh/HC11 *in vivo* transplantation experiments^a

	Cleared fat pad ^{b,c} HC11		Filled fat pad ^{b,d} HC11	
	Int6sh/HC11	Int6sh/HC11	Int6sh/HC11	Int6sh/HC11
Number of mice	18	18	16	16
Number of growths	0	2	0	3

^aNo growths were seen with HC11 cells alone. ^bInjections of 2×10^6 cells were done bilaterally into BALB/c mice; HC11 cells in right #4 mammary gland and Int6sh transfected HC11 cells in the left #4 mammary gland. ^cBALB/c mice were approximately 21 days old. ^dBALB/c mice were retired breeders, approximately 1 year of age

treatment in transplants of MCF10A cells (control) in any of these experiments. This result is consistent with published results for MCF10A cell growth *in vivo* (Pauley *et al.*, 1993).

A similar set of transplantation experiments was conducted with Int6sh-transformed HC11 cells. The transplant hosts were observed for 6 months (Table 2). In the first experiment, Int6sh transfected HC11 cells were injected subcutaneously into the left intact #4 mammary fat pad of retired BALB/c breeders. The

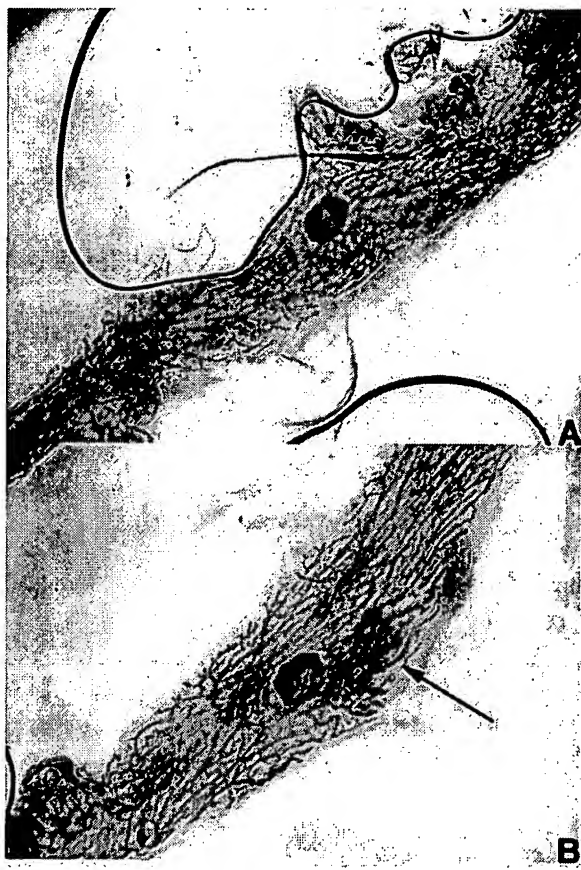


Figure 7 Whole mounts of *in vivo* transplants into BALB/c mice. To test the capacity of Int6sh-transformed cells to generate cellular growths *in vivo*, cells were transplanted into filled mammary glands of retired BALB/c breeders. (a) Filled mammary gland inoculated with HC11 cells (1.6 \times), (b) Filled mammary gland inoculated with Int6sh transfected HC11 cells (1.6 \times). Arrow denotes epithelial growth initiated by inoculated Int6sh-transfected HC11 cells indicative of their capacity to grow within the pad despite the presence of a fully developed host mammary gland.

contralateral right intact #4 mammary fat pad was injected with non-transfected HC11 cells that served as an internal negative control. The mice were observed for 6 months for tumor growth. Thereafter, whole mounts of the mammary glands were made and examined for cellular structures distinct from endogenous structures near the lymph node injection site (Figure 7). Groups of cells were found in three out of 16 Int6sh/HC11 implants that resembled clusters of grapes and were unlinked to the endogenous mammary ductal or alveolar structures. In the second experiment, BALB/c weanlings (ca. 21 day old) had their #4 mammary fat pads cleared of endogenous epithelium and were then injected with the 2×10^6 Int6sh/HC11 cells (left #4 mammary gland) and a similar number of HC11 cells (right #4 mammary gland). Two out of the 18 mice exhibited mammary hyperplastic nodule growths from injections of Int6sh transfected HC11 cells. No epithelial nodules were seen with HC11 cells

alone in either BALB/c experiment. These results demonstrate that Int6sh-transformed HC11 cells are capable of producing epithelial growths in both intact and epithelium-divested mammary fat pads whereas HC11 cells were not. It is significant that Int6sh-transformed HC11 cells are able to produce growths in intact mammary glands because this is an indication of the capacity of these cells to overcome local growth regulatory control in a manner similar to premalignant mammary epithelial cells. We did not expect the non-transformed HC11 cells to grow under these conditions and they did not. In the second experiment, where the fat pads were divested of host epithelium prior to introduction of the cells, we anticipated a greater number of growth takes with an increase in the background for non-transformed HC11 growth *in vivo*. However, there was no positive growth of HC11 cells in these cleared fat pads. Int6sh-transformed HC11 cells however were successful in producing growths in roughly 10% of the implants.

Discussion

Integration of MMTV DNA into the mouse Int6 locus resulting in a truncation of the gene product was found in several independent mouse mammary tumors. This mutation was also present in a premalignant lesion induced by MMTV. All of these transformed mammary populations were clonal in origin suggesting that this truncating mutation to the Int6 gene was relevant to the neoplastic transformation of the affected cell. In this study, we have demonstrated that the expression of a truncated form of the Int6 gene RNA transcript in MCF10A or HC11 mammary epithelial cells and NIH3T3 embryo fibroblasts results in transformation *in vitro* from anchorage dependent to anchorage independent growth. Thus, the *in vitro* transforming activity of truncated Int6 was manifest in both epithelial and mesenchymal cells. A strong association between high steady state levels of Int6sh RNA transcript and clonal anchorage independent growth was established.

Transplantation of the Int6sh-transformed MCF10A and Int6sh transfected HC11 cells demonstrated that these cells had an increased capacity to produce epithelial growths *in vivo*. These data provide direct evidence that the Int6sh mutations found in MMTV-induced mouse mammary premalignant hyperplasia and in mammary tumors directly contribute to their neoplastic transformation. Notably, transformation to frank malignancy was not supported by the expression of Int6sh alone. This observation is consistent with the discovery of the mutation in a premalignant mammary lesion.

Reports have indicated that Int6 is variously associated with eukaryotic translation initiation factor, eIF3, the 43S preinitiation complex, intranuclear RNP particles and elements of the perinuclear Golgi apparatus. A recent report resolves the conflicting literature concerning the subcellular localization of

Int6/eIF3-p48 (Desbois *et al.*, 1996; Diella *et al.*, 1997; Neuveut *et al.*, 1997). Desbois *et al.* (1996) localized Int6 to the PML nuclear bodies, which differed from the observations of Diella *et al.* (1997) that placed Int6 in the Golgi region in the cytoplasm. Int6/eIF3-p48 was recently found to contain two cellular localization signals, a bipartite nuclear localization signal and a nuclear export signal (NES) (Guo and Sen, 2000). The nuclear localization signal (NLS) is located in the midregion (amino acids 264–445) of Int6/eIF3-p48 while the NES is located at the far end of the amino terminus (leucines 6, 14 and 18) (Figure 1B). Desbois *et al.* (1996) used an Int6 fusion protein containing a Flag epitope tag that replaced the first eight N-terminal amino acids to determine the intracellular location of Int6. This effectively deleted the nuclear export signal from the Int6 fusion protein and explains their observation of the epitope-tagged-Int6 localized in the nucleus. The latest evidence has also identified a new potential activity domain within Int6/eIF3-p48, titled the Proteasome-COP9 complex Initiation (PCI) or Proteasome-Int6-Nip1-Trip15 (PINT) motif. This suggests an interaction of Int6 with components in the proteasome/COP9 pathway (Aravind and Ponting, 1998; Hofmann and Bucher, 1998; Karniol *et al.*, 1998; Wei and Deng, 1999). However, to date no direct evidence supports the exact biological significance of the PCI/PINT domain in the Int6 protein. These data imply Int6 may perform multiple functions in cellular processes unrelated to translation initiation. Since truncated Int6 does not contain the nuclear localization signal, we postulate that it may be more prominently effective in the cytoplasm as opposed to the nucleus and that it acts in a dominant fashion. Int6sh induces cellular changes even when two functional alleles are present in the affected cell.

Recent work upon Int6 null and Int6 wild type overexpressing *Saccharomyces pombe* lines correlate with our findings and hypotheses. An Int6 homolog was found in fission yeast (Bandyopadhyay *et al.*, 2000; Crane *et al.*, 2000). The yeast Int6 protein was found strongly associated with 40S ribosomal particles suggesting a common role with mammalian Int6 in translation initiation. Deletion of Int6 from the yeast did not result in a lethal phenotype and only a moderate inhibition of global protein synthesis was observed in its absence. Polysome profiles from the Int6^{-/-} yeast indicated no defect in translation initiation. However, other phenotypes were observed, including slower growth, cell elongation and caffeine sensitivity. These deficiencies were cured by expression of wild type Int6 in the ^{-/-} mutants. The authors concluded that Int6 was not essential for translation initiation in fission yeast. Notably, introduction of human Int6 (identical to the mouse gene) suppressed the slower growth of the Int6 gene-deleted yeast, but did not relieve the other phenotypes. Therefore mammalian Int6 is at least partially functional in yeast. In addition, expression of yeast Int6, with a C-terminus truncation of 50 amino acids, in the wild type cells resulted in increased caffeine sensitivity similar but

more severe than that observed in the gene-deleted strain. The authors postulate that Int6 may be required for translation of a specific set of proteins that effect membrane structure and function, the absence or reduction of these might result in aberrant membrane functions such as endocytosis or transmission of intercellular signals.

Int6sh displays a transformed phenotype similar to that seen in the oncogenic properties of other truncated proteins. The High Mobility Group I (splice variant C) protein (HMGI-C) proteins belong to a group of DNA-binding proteins, which are abundant, heterogeneous, nonhistone components of chromatin (Grosschedl *et al.*, 1994). HMGI-C genes often contain C-terminal truncations that induce neoplastic transformation of NIH3T3 murine fibroblasts (Fedele *et al.*, 1998). HMGI-C truncations and chimeras have transforming activity on NIH3T3 fibroblasts, are able to grow in soft agar, and to induce tumors when inoculated into athymic mice. Fedele *et al.* (1998) postulate that HMGI-C truncations interfere in a dominant fashion with the activity of those transcription factors that are dependent upon HMGI-C thereby inducing transformation. Another example of neoplastic transformation by truncation is with Notch-1. Notch-1 truncations are associated with transformation in Moloney MuLV-infected MMTV^D/myc transgenic mice (Girard and Jolicoeur, 1998). Several tumors, containing a Notch1 rearrangement, over expressed full length Notch1 RNA and protein. However, full length Notch1 was eventually not directly involved in transformation of tumors harboring a provirally activated truncated Notch1 allele.

HC11 cells, which are transformed to anchorage-independent growth by Int6sh, do not possess a functional wild type p53 allele. Nonetheless, Int6sh-transformed HC11 cells did not form tumors when injected into immune-compromised hosts. In mouse mammary tumors, the Int6 gene promoter drives expression of the shortened Int6 allele. We have no information regarding the transcriptional control of Int6, however it appears to be constitutive in non-cycling tissue. In the HOG and tumors, the Int6sh transcript ends in the MMTV LTR promoter but in our system no MMTV sequences are present, suggesting that there may be no contribution of the MMTV sequences to the transforming activity of truncated Int6.

Marchetti *et al.* (2001) recently published a study, which investigated the frequency of Int6 mutations in human breast and lung carcinomas. They cited evidence for a concomitant reduction of Int6/eIF3-p48 expression in a subset of human breast and lung carcinomas. In addition, a relationship was established between decreased expression of Int6/eIF3-p48 and tumor histotype in non-small cell lung carcinomas, which are almost exclusively adenocarcinomas. Thus, it is tempting to postulate that loss of normal Int6/eIF-p48 deregulates a critical cellular pathway (translation and/or proteasome) and leads to neoplastic transformation. However, additional work is needed to

elucidate the pathways that are directly affected by perturbation of Int6/eIF3-p48 expression and induction of neoplastic transformation.

In conclusion, we have taken a first step toward demonstrating that expression of a truncated form of the Int6 gene transcript may result in partial transformation of the affected cell. Our longer-term approach to this question has resulted in the creation of a transgenic mouse model where Int6sh is expressed in the mammary glands from the mouse Whey Acidic Protein (WAP) promoter. Presently we have developed 11 independent founder lines but have only found expression of the transgene in the lactating mammary tissue of two of these families. We are currently force-breeding females from these expressing lines to determine whether hyperplasia or tumors will appear in the affected mammary tissues. Of interest is a male founder line where two of the F1 sibling males have developed testicular masses and have failed to breed successfully. A 1995 study of WAP promoter expression in male mice indicates that WAP is expressed constitutively in the testes, however the precise cellular locale of WAP expression within the testis has not been ascertained (Wen *et al.*, 1995). We are currently determining if these testicular lesions are associated with the expression of the transgene.

Materials and methods

Antibodies

As described previously (Diella *et al.*, 1997), polyclonal antibodies against the synthetic peptides #20 (KDVRKRRQVLKDLVKVIQQE) and #47 (YKNLYSD-DIPHLREK) of Int6 were used in immunoprecipitation and Western immunoblot. The epitope of antibody #47 (Int6 #47) is located at the N-terminus of Int6 while antibody #20's epitope is found towards the Int6 C-terminus. Thus, Int6 #20 antibody does not recognize the Int6sh protein (see Figure 1). In addition, commercially available monoclonal and polyclonal HA.11 (Babco/Covance, Berkley, CA, USA) against hemagglutinin were also used in Western immunoblots.

Enzymes

All restriction endonucleases were purchased from Boehringer Mannheim (Indianapolis, IN, USA) or Promega (Madison, WI, USA) and used according to manufacturer's specifications.

Oligonucleotides

All DNA oligomers were purchased from either IDT (Coraville, IA, USA) or Life Technologies (Gaithersburg, MD, USA).

DNA preparation

All DNA plasmid preparations were performed according to the established protocols by Sambrook *et al.* (1989). Plasmid preparations were facilitated through the use of either the Wizard™ miniprep DNA purification system, a commercial kit from Promega (Madison, WI, USA) or Qiaprep™

miniprep DNA purification system, a commercial kit from Qiagen, Inc (Chatsworth, CA, USA). DNA used for transfection was purified using standard CsCl techniques by Lofstrand Labs Inc (Gaithersburg, MD, USA). DNA fragment preparations were simplified through the use of the Qiaex II Gel Extraction Kit, a commercial kit from Qiagen Inc. (Chatsworth, CA, USA).

Recombinant Int6sh gene construction

Two oligonucleotides of approximately 30 bp were used along with Int6 cDNA from murine cell lines to amplify a 700 bp region using the polymerase chain reaction (PCR). Forward primer was DG621-5'-GGT-AAG-CTT-AAC-AAG-CGC-TCC-TTT-CCC-CC-3' and Int6SHREV-5'-GGA-CTT-AAG-GAA-GCC-AGA-GTC-TTG-GGT-TGC-3'. This process generated a synthetic Int6sh gene with flanking HindIII and EcoRI restriction endonuclease sites. Recombinant Int6sh gene was initially identified by restriction analysis. The DNA sequence of the synthetic Int6sh gene was determined and the correct nucleotide sequences confirmed. This HindIII-EcoRI Int6sh DNA fragment was ligated directly into the pCEFLHA vector.

C-terminal green fluorescent protein construction

The Int6sh gene cassette was amplified from Int6sh-pCEFLHA vector using two primers of approximately 20 bp. Int6Start_For-5'-TCC-CCC-GGC-AAG-ATG-GCG-G-3'; HA1_Rev-5'-CGT-AAT-CCG-GTA-CGT-CAT-3'. This synthetic Int6sh-HA PCR product was then ligated to the pCDNA3.1/CT-GFP-TOPO vector according to manufacturer's protocol.

Ligation and transformation reactions

Ligation and transformation reactions were done according to published procedures in Sambrook *et al.* (1989). The only deviation from published procedure was done according to the recommended protocol provided by the manufacturer regarding the particular bacterial host and commercial source of T₄ DNA Ligase.

PCR analysis for Alu sequences

Genomic DNA was extracted from tissue using Qiagen's QiAmp Kit as per protocol for paraffin embedded tissue. The primer set used for Alu sequences was SBR13 (For), 5'-GCCTGTAATCCCAGCACTT-3' and SBR14 (Rev), 5'-CCGGGTTCACGCCATT-3'. Annealing temperature was 59°C with a product of 188 bp. Utilized Easystart™ 100 PCR Mix in a Tube (Molecular BioProducts, San Diego, CA, USA). Mouse Cot-1 DNA (Gibco-BRL) was used as negative control and Human Cot-1 DNA (Gibco-BRL) was used as the positive control.

Expression plasmids

The synthetic Int6short gene was ligated into the pCEFLHA vector (Omar Coso) and transformed into DH5 α cells (Gibco-BRL, Gaithersburg, MD, USA). DNA sequences were verified using dye terminator sequencing on an ALF automated sequencer. The pCEFLHA transfection vector has the backbone of pCDNA® 3.0(+) (Invitrogen, Carlsbad, CA, USA) with several modifications. The cytomegalovirus (CMV) promoter was replaced by eukaryotic elongation factor-1 alpha promoter (eEF1A). The multiple cloning site

was altered to accommodate the HA epitope tag. This vector contains the Neo^R gene that allows selection of stable transfecants using G418 sulfate. This vector was obtained from Dr Omar Coso. To express truncated Int6, a vector was constructed from the pCDNA 3.1(+) backbone, replacing the cytomegalovirus (CMV) promoter with elongation factor 1-alpha (eEF1A) promoter and adding a hemagglutinin (HA) epitope tag for protein identification purposes. This promoter has previously been used to drive expression of genes in a wide range of cell types *in vitro* (Goldman *et al.*, 1996; Mizushima and Nagata, 1990).

For the C-terminal green fluorescent fusion protein, the pCDNA3.1/CT-GFP-TOPO vector (Invitrogen, Carlsbad, CA, USA) was utilized to ligate the synthetic Int6sh-HA PCR product. This vector also contains the Neo^R and Amp^R gene.

Transfection conditions

MCF-10A, HC11 or NIH3T3 cells were grown to 80% confluence in a 75 cm² flask. The cells were then trypsinized and seeded at a ratio of approximately 10⁶-cells/60 mm dish/5 ml of cell culture medium. Cells were allowed to grow overnight in 5% CO₂, 37°C. The following day, cells were transfected with appropriate vector using the commercial liposomal reagent DOTAP™ from Boehringer Mannheim/Roche.

In vitro translation and immunoprecipitation of Int6 short and Int6 wild type

Equal amounts (1 µg) of Int6sh and Int6 wild type vectors were *in vitro* translated using the TnT Coupled Reticulocyte System (Promega, Madison WI, USA) with [³⁵S]Methionine. Ten microliters of the *in vitro* translation reaction mixture was immunoprecipitated with each of three antibodies, monoclonal and polyclonal HA.11 (Babco/Covance) and Int6 #47 polyclonal antibodies, utilizing protein G agarose (Boehringer Mannheim/Roche Indianapolis, IN, USA). The HA.11 antibodies (Babco/Covance, Berkley, CA, USA) recognize the C-terminal hemagglutinin epitope tag and the Int6 #47 antibody recognizes the N-terminus of Int6 (Diella *et al.*, 1997). The antibody-protein G-agarose pellet was washed as per manufacturer's protocol and eluted into 50 microliters of 1× SDS-PAGE loading dye for direct loading upon an SDS-PAGE gel.

Cell lines and culture conditions

MCF-10A cells (Soule *et al.*, 1990), a normal human mammary epithelial cell line, were cultured in DMEM/F-12 (1:1) supplemented with 5% equine serum (heat inactivated; Gemini BioProducts, Calabassas, CA, USA), 2 mM glutamine (Gibco-BRL, Gaithersburg, MD, USA), 20 mM HEPES (Gibco-BRL), 100 ng/ml of cholera toxin (List Biological Laboratories, Campbell, CA, USA), 10 µg/ml of insulin (Gibco-BRL), 500 ng/ml of hydrocortisone (Sigma Chemical Co., St. Louis, MO, USA), and 10 ng/ml of recombinant mouse EGF (Collaborative Biomedical Products, Bedford, MA, USA). Cells are grown in 5% CO₂ at 37°C. HC11 cells, a normal mouse mammary epithelial cell line, were cultured in RPMI 1640 supplemented with 10% fetal bovine serum (heat inactivated; Gemini BioProducts), 2 mM glutamine, 5 µg/ml of insulin, and 10 ng/ml of recombinant mouse EGF. NIH3T3 cells, a normal mouse embryo fibroblast cell line, were cultured in DMEM supplemented with 10% fetal bovine serum (heat inactivated;

Gemini BioProducts). All cell lines are routinely passaged in media containing penicillin-streptomycin at a final concentration of 1× (Gibco-BRL). Cell lines that were selected for Neomycin resistance were initially culture in 750 µg/ml Neomycin sulphate until stable lines were created. Afterwards, these cell lines were maintained in 350 µg/ml Neomycin sulphate. Doubly-transformed DBL/NIH3T3 cells and Harvey Ras-transformed MCF10A cells (MCF10AneoT) were provided by Dr David Salomon, LTIB, NCI as a positive control for anchorage independent growth in soft agar (Ciardiello *et al.*, 1990a,b, 1992; Normanno *et al.*, 1994). These transformed cell lines were cultured in conditions identical to that of their originating cell lines, NIH3T3 and MCF10A respectively.

Immunocytochemistry

Int6sh-CTGFP/NIH3T3 cells were seeded onto 22 mm square glass cover slips in a six-well plate and cultured in DMEM supplemented with 10% FBS. All steps were performed at room temperature unless noted otherwise. After washing twice in PBS, cells were fixed with 3.5% paraformaldehyde in PBS for 10 min and then permeabilized with 0.5% Triton X-100 in PBS for 10 min. The wash solution contained 0.1% Tween 20 and 10% FBS in PBS. Cells were then washed once and then incubated with a 1:1000 dilution of monoclonal GFP antibody (Covance), diluted in wash solution, for 3 h. Coverslips were then washed once and then incubated with goat anti mouse FITC conjugated secondary antibody (1:250, Santa Cruz Biotechnology, Santa Cruz, CA, USA) containing DAPI (1:50 000, Molecular Probes) in wash solution for 2 h. Coverslips were then washed twice and then rinsed twice in distilled water. Coverslips were mounted onto standard microscope slides using Prolong Antifade mounting media (Molecular Probes). Cells were visualized using a standard Nikon Eclipse TE300 microscope and 100× objective with 5000 ms exposure. Filter set used was 403/460 nm for DAPI and 492/520 nm for FITC.

Soft agar growth assay

A stock solution of 2.7% SeaKem GTG agar in ddH₂O was prepared and autoclaved for 20 min. Agar was then cooled in a 65°C bath. For the base layer, the agar stock solution was mixed with medium to reach a final concentration of 0.9% and allocated at 1 ml/35 mm dish. The base layer was allowed to cool and solidify for 30 min. A top agar containing 0.34% agar was prepared in a similar manner, with cells added to the top agar at a final concentration of either 15 000 or 30 000 cells/ml/dish. Two ml of this mixture was layered on top of the base layer and allowed to solidify for 30 min–1 h before placing dishes into a 37°C, 5% CO₂ incubator. Plates were grown for 3–4 weeks or until colonies were apparent. The day before counting colonies, stain with 1 ml/well of nitroblue tetrazolium (50 mg NBT in 100 ml PBS). Colonies were counted using an Artek camera system.

Cell lysis and fractionation protocol

Cells, at 80–90% confluence in a 75 cm² flask, were washed twice in cold PBS. Then, 1 ml of lysis buffer (50 mM Tris, pH 7.5, 2 mM EDTA, 1% Triton X-100, 100 mM NaCl) was added to the cells, and the cells were subsequently scraped into solution using a plastic cell lifter (Costar® Corp., Cambridge, MA, USA). This mixture was then mixed in

equal amounts with 2× SDS loading buffer and analysed by denaturing SDS-PAGE electrophoresis.

Sodium dodecyl sulfate polyacrylamide gels (SDS-PAGE)

All SDS-PAGE gels were purchased from either Novex (San Diego, CA, USA) or BioRAD (Hercules, CA, USA) and electrophoresed according to the protocols listed in Sambrook *et al.* (1989). The protein gels used a Tris-Glycine buffering system.

Western immunoblot analysis

Western immunoblot detection of Int6 protein followed the procedure of Towbin *et al.* (1979). A polyclonal antiserum against the Int6 #20 peptide was used as the primary antibody. Sheep anti-rabbit IgG antiserum conjugated to horseradish peroxidase (Amersham, Arlington Heights, IL, USA) was used as the secondary antibody. Immunoblots were developed using chemiluminescent reagents provided in the ECL kit also from Amersham. Bands were visualized using autoradiographic film at varying exposure times.

Protein concentration determination

Protein concentrations were determined using the BioRAD Protein Assay kit (BioRAD, Hercules, CA, USA). Serial dilutions of bovine plasma gamma globulin (BioRAD standard I) were used as a protein standard.

In vivo experiments

In vivo experiments were done to assess the tumorigenic potential of Int6sh transfected MCF10A cell lines. In the first experiment, two methods were used for introduction of the

transfected cells *in vivo* (2×10^6 cells/10 µl injection in PBS). One-year-old athymic (nu/nu) mice were subcutaneously injected directly into the L4 mouse mammary fat pad distal to the lymph node; 30 mice were utilized for experimental cells (three different clones) and 10 for the control group (MCF10A). The second method involved an intrascapular injection of a 1:1 mixture of Int6sh/MCF10A cells and Matrigel®. Ten mice per experimental group were used (three independent clones of Int6sh/MCF10A and one control MCF10A group).

Based on the first experiment, a second *in vivo* experiment was performed with athymic mice. The mice were injected subcutaneously near the #4 mammary nipple with a 1:1 mixture of cells and Matrigel®. Each injection contained 10^7 cells.

A third *in vivo* experiment was performed using Int6sh/HC11 cells. First, injections were done into the L4 mammary fat pads of BALB/c mice, whose ages were at least 12 months or more; the contralateral R4 mammary fat pad was injected with HC11 cells, which are serving as an internal negative control. Each injection contained 2×10^6 cells in 100 µl of media. Second, BALB/c weanlings had their #4 mammary fat pads cleared and then injected in the same fashion as listed above for the yearlings.

Acknowledgments

We are indebted to Dr Omar Coso for the generous gift of the pCEFLHA vector and Dr Chris Baumann for his tireless work in visualizing the Int6 wild type and Int6sh-GFP fusion proteins. Brenda Jones in Dr D Salomon's laboratory for providing the transformed cell lines for anchorage-independent growth studies. We would also like to thank Dr Mary Hilburger-Ryan and Dr David Salomon for critical reading of this manuscript.

References

- Aravind L and Ponting CP. (1998). *Protein Sci.*, **7**, 1250–1254.
- Asano K, Krishnamoorthy T, Phan L, Pavitt GD and Hinnebusch AG. (1999). *EMBO J.*, **18**, 1673–1688.
- Asano K, Merrick WC and Hershey JWB. (1997a). *J. Biol. Chem.*, **272**, 23477–23480.
- Asano K, Vornlocher H-P, Richter-Cook NJ, Merrick WC, Hinnebusch AG and Hershey JWB. (1997b). *J. Biol. Chem.*, **272**, 27042–27052.
- Bandyopadhyay A, Matsumoto T and Maitra U. (2000). *Mol. Biol. Cell*, **11**, 4005–4018.
- Ciardiello F, Gottardis M, Basolo F, Pepe S, Normanno N, Dickson RB, Bianco AR and Salomon DS. (1992). *Mol. Carcinog.*, **6**, 43–52.
- Ciardiello F, McGeady ML, Kim N, Basolo F, Hynes N, Langton BC, Yokozaki H, Saeki T, Elliott JW, Masui H, Mendelsohn J, Soule H, Russo J and Salomon DS. (1990a). *Cell Growth Differ.*, **1**, 407–420.
- Ciardiello F, Valverius EM, Colucci-D'Amato GL, Kim N, Bassin RH and Salomon DS. (1990b). *J. Cell Biochem.*, **42**, 45–57.
- Crane R, Craig R, Murray R, Dunand-Sauthier I, Humphrey T and Norbury C. (2000). *Mol. Biol. Cell*, **11**, 3993–4003.
- Desbois C, Rousset R, Bantignies F and Jalinot P. (1996). *Science*, **273**, 951–953.
- Diella F, Levi G and Callahan R. (1997). *DNA Cell Biol.*, **16**, 839–847.
- Fedele M, Berlingieri MT, Scala S, Chiariotti L, Viglietto G, Rippel V, Bullerdiek J, Santoro M and Fusco A. (1998). *Oncogene*, **17**, 413–418.
- Fukuchi-Shimogori T, Ishii I, Kashiwagi K, Mashiba H, Ekimoto H and Igarashi K. (1997). *Cancer Res.*, **57**, 5041–5044.
- Girard L and Jolicoeur P. (1998). *Oncogene*, **16**, 517–522.
- Goldman LA, Cutrone EC, Kotenko SV, Krause CD and Langer JA. (1996). *Biotechniques*, **21**, 1013–1015.
- Grosschedl R, Giese K and Pagel J. (1994). *Trends Genet.*, **10**, 94–100.
- Guo J and Sen GC. (2000). *J. Virol.*, **74**, 1892–1899.
- Hershey JW. (1991). *Annu. Rev. Biochem.*, **60**, 717–755.
- Hofmann K and Bucher P. (1998). *Trends Biochem. Sci.*, **23**, 204–205.
- Jurka J and Milosavljevic A. (1991). *J. Mol. Evol.*, **32**, 105–121.
- Karniol B, Yahalom A, Kwok S, Tsuge T, Matsui M, Deng XW and Chamovitz DA. (1998). *FEBS Lett.*, **439**, 173–179.
- Lazaris-Karatzas A, Montine KS and Sonenberg N. (1990). *Nature*, **345**, 544–547.
- Lazaris-Karatzas A and Sonenberg N. (1992). *Mol. Cell Biol.*, **12**, 1234–1238.
- MacPherson I and Montagnier L. (1964). *Virology*, **23**, 291–294.
- Marchetti A, Buttitta F, Miyazaki S, Gallahan D, Smith GH and Callahan R. (1995). *J. Virol.*, **69**, 1932–1938.

- Marchetti A, Buttitta F, Pellegrini S, Bertacca G and Callahan R. (2001). *Int. J. Oncol.*, **18**, 175–179.
- Methot N, Song MS and Sonenberg N. (1996). *Mol. Cell. Biol.*, **16**, 5328–5334.
- Miyazaki S, Imatani A, Ballard L, Marchetti A, Buttitta F, Albertsen H, Nevanlinna HA, Gallahan D and Callahan R. (1997). *Genomics*, **46**, 155–158.
- Miyazaki S, Kozak CA, Marchetti A, Buttitta F, Gallahan D and Callahan R. (1995). *Genomics*, **27**, 420–424.
- Mizushima S and Nagata S. (1990). *Nucleic Acids. Res.*, **18**, 5322.
- Neuveut C, Jin D-Y, Semmes OJ, Diella F, Callahan R and Jeang K-T. (1997). *J. Biomed. Sci.*, **4**, 229–234.
- Normanno N, Selvam MP, Qi CF, Saeki T, Johnson G, Kim N, Ciardiello F, Shoyab M, Plowman G, Brandt R, Todaro G and Salomon DS. (1994). *Proc. Natl. Acad. Sci. USA*, **91**, 2790–2794.
- Nupponen NN, Isola J and Visakorpi T. (2000). *Genes Chrom. Cancer*, **28**, 203–210.
- Nupponen NN, Porkka K, Kakkola L, Tanner M, Persson K, Borg A, Isola J and Visakorpi T. (1999). *Am. J. Pathol.*, **154**, 1777–1783.
- Pauley RJ, Soule HD, Tait L, Miller FR, Wolman SR, Dawson PJ and Heppner GH. (1993). *Eur. J. Cancer Prev.*, **2** (Suppl 3), 67–76.
- Pestova TV, Hellen CUT and Shatsky IN. (1996). *Mol. Cell. Biol.*, **16**, 6859–6869.
- Sambrook J, Fritsch EF and Maniatis T. (1989). *Molecular cloning: a laboratory manual*, 2nd edn. Cold Spring Harbor Laboratory, Cold Spring Harbor, NY.
- Soule HD, Maloney TM, Wolman SR, Brenz R, McGrath CM, Russo J, Pauley RJ, Jones RF and Brooks SC. (1990). *Cancer Res.*, **50**, 6075–6086.
- Towbin H, Staehelin T and Gordon J. (1979). *Proc. Natl. Acad. Sci. USA*, **76**, 4350–4354.
- Wei N and Deng XW. (1999). *Trends Genet.*, **15**, 98–103.
- Wen J, Kawamata Y, Tojo H, Tanaka S and Tachi C. (1995). *Mol. Reprod. Dev.*, **41**, 399–406.

**This Page is Inserted by IFW Indexing and Scanning
Operations and is not part of the Official Record**

BEST AVAILABLE IMAGES

Defective images within this document are accurate representations of the original documents submitted by the applicant.

Defects in the images include but are not limited to the items checked:

- BLACK BORDERS**
- IMAGE CUT OFF AT TOP, BOTTOM OR SIDES**
- FADED TEXT OR DRAWING**
- BLURRED OR ILLEGIBLE TEXT OR DRAWING**
- SKEWED/SLANTED IMAGES**
 - COLOR OR BLACK AND WHITE PHOTOGRAPHS**
- GRAY SCALE DOCUMENTS**
- LINES OR MARKS ON ORIGINAL DOCUMENT**
- REFERENCE(S) OR EXHIBIT(S) SUBMITTED ARE POOR QUALITY**
- OTHER:** _____

IMAGES ARE BEST AVAILABLE COPY.

As rescanning these documents will not correct the image problems checked, please do not report these problems to the IFW Image Problem Mailbox.